BOWING AND CORRESPONDING THERMAL STRESS PHENOMENA IN FUEL PINS DURING TRANSIENTS

J. P. HALLEUX, J. REYNEN

Commission of the European Communities,
EURATOM JRC, Applied Mechanics Division, I-121020-Ispra (Varese), Italy

SUMMARY

Although the thermal mechanical behaviour of fuel pins has been studied in detail for steady-state conditions, much less attention has been paid to these problems during transients.

The present paper deals with bowing and thermal stress phenomena in fuel pins during blow-down transients.

For this purpose the volumetric heat generation Q in the cross-section of the fuel pin is approximated as:

$$Q(r,\theta,t) = \frac{p(t)}{\pi a^2\left(1+\frac{\alpha}{2}\right)}\left[1+\gamma\left(\frac{r}{a}\right)\cos\theta\right]\left[1+\alpha\left(\frac{r}{a}\right)^2\right]$$

r, θ cylindrical coordinates,
$p(t)$ local linear power as function of time,
a fuel pellet radius,
γ circumferential tilting factor,
α radial depression factor.

By means of FEM the transient circumferential temperature distribution is analysed in a zircalloy cladded UO_2 fuel pin, for a representative spectrum of parameters. The transient heat transfer coefficient at the outer-cladding wall are obtained from out-of-pile flow-down experiments. Solutions for both temperature dependent and independent material properties are given.

The results show that the circumferential temperature variations in the canning are more pronounced during transients as compared to steady-state conditions. The influence of the gap resistance remains small. Thermal stresses and related fuel pin bowing phenomena remain within acceptable limits.

1. Introduction

At the Joint Research Centre (JRC, Euratom) of the European Communities, at Ispra (Italy), a project is going on, sponsored by the Italian Government, to carry out LWR in-pile accident simulations. For this purpose various loops are under construction in the ESSOR reactor. This reactor, originally being built as a testing reactor for various technical aspects of the concept of pressure tube reactors (ORGEL, organic cooled, heavy water moderated) is particularly suited for such modifications.

The ESSOR reactor (Fig. 1) consists of a tank filled with heavy water. The tank is penetrated by through-through channels in vertical direction in which the pressure tubes can be mounted. Although the ORGEL project with organic liquid as coolant had a nominal pressure of about 20 bars, a careful design makes it possible to introduce into some existing holes demountable loops representative for LWR fuel bundles (i.e. BWR 90 bar, PWR 180 bar). In these loops it will be possible to test candidate fissile fuels in the form of either a single pin or bundles, including such phenomena as partial channel blockage, cladding defects, simulation of LOCA, dry-out, reflooding, etc.

The neutronics of such a heterogeneous reactor core have revealed [1] that the thermal neutron flux tilting factor γ and the radial depression factor α depend strongly on the position of the channel in the main tank and can differ significantly from those in current LWR designs.

In the present paper a FEM analysis is presented to study the effects of the power tilting on the thermal-mechanical behaviour of the fuel pin during blow-down conditions.

2. Analysis

2.1 Differential Equation

The temperature distribution in fuel and cladding (Fig. 2) is governed by:

$$
\begin{aligned}
&\nabla \lambda_1 \nabla T - (\rho c)_1 \frac{\partial T}{\partial t} = -Q && \text{fuel} && 0 \leq r \leq a \\
&\nabla \lambda_2 \nabla T - (\rho c)_2 \frac{\partial T}{\partial t} = 0 && \text{canning} && a \leq r \leq b \\
&-\lambda_1 \frac{\partial T}{\partial r} = -\lambda_2 \frac{\partial T}{\partial r} = h_g (T_{a,1} - T_{a,2}) && \text{gap} && r = a \\
&-\lambda_2 \frac{\partial T}{\partial r} = h_f (T_b - T_m) && \text{film} && r = b
\end{aligned}
\qquad (1)
$$

$T(r, \theta, t)$	temperature distribution [°C]
λ	conductivity [W/cm°C]
ρc	thermal inertia [Wsec/cm^3°C]
r, θ, t	coordinates, time [cm, sec]
a, b	fuel pin dimensions [cm] (Fig. 2)
h_g	gap heat transfer coefficient [W/cm^2°C]
h_f	film heat transfer coefficient [W/cm^2°C]
Q	heat generation [W/cm^3]

1, 2 subscripts referring to fuel, resp. canning

T_m bulk temperature [°C]

The heat generation Q which will be considered, has the form:

$$Q(r,\theta,t) = \frac{p(t)}{\pi a^2 (1+\frac{\alpha}{2})} \left(1 + \gamma(\frac{r}{a})\cos\theta\right)\left(1 + \alpha(\frac{r}{a})^2\right) \tag{2}$$

where p(t) is the so-called linear power

$$p(t) = \int_0^{2\pi}\int_0^a Q(r,\theta,t)\, r\, dr\, d\theta. \tag{3}$$

2.2 Analytical Steady State Solution. Stress Analysis

For temperature independent thermal conductivity for both fuel and canning, a closed form solution of the steady state problem can be obtained. The temperature distribution becomes [2]:

$$\frac{T(0,0)}{\bar{T}_b} = 1 + Nu_2 \ln(\frac{b}{a}) + \frac{\lambda_2 Nu_2}{\lambda_1 Nu_1} + \frac{Nu_2}{2+\alpha}\frac{\lambda_2}{\lambda_1}(1+\frac{\alpha}{4})$$

$$\frac{T(r,\theta)}{\bar{T}_b} = 1 - Nu_2 \ln(\frac{r}{b}) + \frac{Nu_2}{2+\alpha}\gamma\left(F_1(r) + \frac{2}{3}\alpha F_3(r)\right)\cos\theta \qquad \text{for } a \leq r \leq b \tag{4}$$

$$F_n(r) = \frac{(\frac{r}{b})^n (\frac{n}{Nu_2} - 1) + (\frac{r}{b})^{-n} (\frac{n}{Nu_2} + 1)}{(\frac{b}{a})^n (\frac{n}{Nu_2}+1)(\frac{n}{Nu_1} + 1 + \frac{\lambda_1}{\lambda_2}) - (\frac{b}{a})^{-n} (\frac{n}{Nu_2} - 1)(\frac{n}{Nu_1} + 1 - \frac{\lambda_1}{\lambda_2})}$$

where:

$Nu_1 = \frac{h_g a}{\lambda_1}$, $Nu_2 = \frac{h_f b}{\lambda_2}$ Nusselt numbers,

$\bar{T}_b = p(0)/2\pi b h_f$ average outer canning temperature

The canning temperature distribution can be split up into a purely radial one and a circumferential one. The purely radial temperature variation gives rise to thermal stresses which are related to the temperature drop over the canning $\overline{\Delta T}_r$

$$\overline{\Delta T}_r = \bar{T}_b\, Nu_2 \ln(\frac{a}{b}) \tag{5}$$

$$\sigma_{zz} = \sigma_{\theta\theta} = \pm \frac{\beta \overline{\Delta T}_r E}{2(1-\nu)} \tag{6}$$

The circumferential temperature variation gives rise to both thermal stresses and thermal bowing. The bowing of a fuel element is governed by the term proportional to $r\cos\theta$ i.e. a linear field in a cartesian coordinate system, which has to be extracted from eq. (4), for example by the method of least squares. However, since the canning is

thin, it is a good approximation to define the local average (in radial direction) canning temperature and to consider the variation of this quantity over the circumference:

$$\overline{\Delta T_c} = \overline{T_b}\,\frac{2Nu_2}{2+\alpha}\,\gamma\left(F_1\left(\tfrac{1}{2}(a+b)\right) + \tfrac{2}{3}\alpha F_3\left(\tfrac{1}{2}(a+b)\right)\right) \tag{7}$$

The bowing of the canning follows then from classical beam theory:

$$\frac{d^2W}{dz^2} = \frac{\beta\overline{\Delta T_c}}{2b} - \frac{M}{EI}$$

$$W = \frac{\beta\overline{\Delta T_c}}{4b}\,z^2 + Az + B - \iint \frac{M}{EI}\,dz\,dz \tag{8}$$

The integration constants A and B, as well as the moment distribution, follow from boundary conditions due to spacers. In particular when the spacers are placed such that the fuel element remains nearly straight, the upper bound for thermal stress is obtained from an equation like eq. (6), but dropping the factor $(1-\nu)$ because the stress field is monoaxial

$$\sigma_{zz} = \pm\frac{\beta\overline{\Delta T_c}\,E}{2}\,,\quad \sigma_{\theta\theta} = 0 \tag{9}$$

Part of the circumferential term in eq. (4) produces also thermal stresses due to the local radial variation. The corresponding temperature difference can be written as:

$$\Delta T_{r,c} = \overline{T_b}\,\frac{Nu_2}{2+\alpha}\,\gamma\left(F_1(b) - F_1(a) + \tfrac{2}{3}\alpha\left(F_3(b) - F_3(a)\right)\right) \tag{10}$$

For the corresponding thermal stress eq. (6) should be used because of the biaxiality of the stress field.

2.3. FEM Transient Analysis

A closed form solution of eq. (1) for the indicated heat generation term, eq. (2) and a time-dependent linear power p(t) is not possible and recourse is to be made to a numerical method such as FEM.

As a computer program the FEM system FLHE [3] has been used. In a first approach and in order to separate the effect of power tilting, a solution is obtained by assuming temperature-independent thermal properties (conductivity λ, heat capacity ρc). As can be seen from the analytical steady state solution eq. (4) a source term of the form $Q = f(r)\cos n\theta$ gives rise to a temperature distribution of the type $T = T_n(r)\cos n\theta$. For the transient problem with source term $Q = p(t)\,f(r)\cos n\theta$ the resulting temperature distribution can be written as $T = T_n(r,t)\cos n\theta$. This implies that the Fourier terms of order zero and of order one of the heat generation term Q, eq. (2), can be dealt with separately. The zero order term is treated by means of the mesh of Fig. 3a and represents as a matter of fact a 1D transient problem. The first order term ($\cos\theta$) is dealt with by means of the mesh depicted in Fig. 3b with the indicated boundary condition $T = 0$ at $\theta = 90^\circ$.

The gap in both meshes is represented by an eight-noded element with conductivity $\lambda = h_g$/(thickness of gap) and thermal inertia (ρc) equal zero. Since FLHE uses a semi-implicit integration scheme (Crank Nicholson [4]) the fact that the midside node halfway the gap has no thermal inertia does not give rise to numerical difficulties.
Although this mesh looks rather coarse, the confrontation of the numerical steady state solution with the numerical one has revealed good accuracy for low values of the radial depression factor α (Table I). For higher values of α (=.31) the mesh has shown to be too coarse due to the fact that the heat generation term Q in FLHE is to be specified per element, and no option exists yet to specify it per nodal point. Therefore a more refined mesh (Fig. 4) has been used to deal with high radial depression factors. This mesh which covers 180° can be used to deal with the zero and first order term simultaneously, and in this way temperature-dependent conductivity can be employed. The radial mesh enables to calculate exactly the average heat generation per element

$$\bar{Q}_e = \iint Q r \, dr \, d\theta \Big/ \iint r \, dr \, d\theta \qquad (11)$$

The comparison with the closed form steady state solution is made in Table II.

It is seen that even for this more refined mesh the discrepancy in $\overline{\Delta T_c}$ (node 26 - node 50) is still important. It is, however, decided not to refine the mesh but to modify FLHE in order to be able to specify the source term per node with an interpolation by means of the shape functions.

3. Results

The inner and outer rod of a 52-pins fuel bundle under "hot" reference conditions [1] have been analyzed. For the outer rod ($\alpha = 0$, $\gamma = 0.14$) the simplified model has been applied (mesh of Fig. 3); for the inner rod ($\alpha = 0.31$, $\gamma = 0.1$) the more general solution (mesh of Fig. 4) has been used for reasons explained above, enabling also to study the effect of temperature-dependent fuel conductivity.

The fuel pin characteristics are given in Fig. 2 and Table III. The time-dependent source term follows the scram curve (Table IV). During the scram the tilting factor γ is halved according to neutronics calculations [1]. Coolant temperature (Table IV) and heat transfer coefficient (Fig. 5) have been determined experimentally [1] for both a "moderate" and a "fast" blow down. The results are plotted in Figs. 6 and 7 for moderate and fast blow down transients respectively. In Fig. 6 is also included the effect of a 1 sec scram delay.

These results show that the mean circumferential temperature distribution can become of the order of $30^{\circ}C$ ($\alpha = 0$, $\gamma = 0.1$, scram delay 1 sec, $\overline{\Delta T_c} = 30^{\circ}C$) but is well below the nominal radial temperature drop of about $60^{\circ}C$ (Table II). Moreover, the maximum is passed before reaching critical overall temperatures. The moderate blow down gives rise to the largest temperature tilt. Scram delay evidently increases the overall temperature

but also the temperature tilt as follows from Fig. 6. Radial depression of thermal neutron flux does not seem to affect the transient solution more significantly than the steady state solution. A 50% variation of the gap heat transfer coefficient showed almost no effect on the circumferential temperature distribution. Applying formulae (6) and (9) it is seen that the stress level due to a 30°C circumferential temperature variation as compared to a 60°C radial temperature drop is a factor $2/(1-\nu) \cong 3$ lower, which means that the thermal stress could increase by 30% maximum:

$$\sigma_{zz} = \frac{\beta E}{2}\left(\frac{60}{1-\nu} + 30\right) = 2.73 + 0.95 = 3.68 \text{ kg/mm}^2.$$

However, by the time the 30° circumferential temperature variation is reached the radial temperature drop is decreased significantly.

4. Conclusions

Finite element techniques have shown to be of great help to deal with detailed temperature distributions in fuel pins. In order to describe accurately accentuated spatial variations of heat generation an option should exist to specify the source term per node rather than per element.

Concerning the presented problem it can be concluded that the magnification of azimuthal temperature distributions during transients only slightly increases the thermal stress level.

Acknowledgement

The authors are indebted to Messrs. Blanckenburg and De Windt who have been in charge of the computer runs.

References

[1] FRIZ, G., RANDLES, J., RIESCH, G., Euratom JRC-Ispra, ESSOR Project, Private Communication

[2] ARANOVITCH, E., LABARRE, E., REYNEN, J., "Etudes des perturbations circonférentielles et axiales de température dans une gaine cylindrique d'élément combustible", EUR Report 2480.f (1965)

[3] FULLARD, K., "FLHE, A Finite Element Program for the Calculation of Temperatures in Arbitrary Structures", CEGB Rep. RD/B/N1849

[4] CRANK, J., NICHOLSON, P., "A Practical Method for Numerical Integration of Solution of Partial Differential Equations of Heat Conduction Type", Proc. Cambridge Philosophical Soc., vol. 43, page 50 (1947).

TABLE I

	r=b	$r=a_+$	$r=a_-$	r=0
analytical(+312.16)°C	46.56	105.6	447.2	1614
numerical(+312.16)°C	46.56	100.4	439.9	1607
$\alpha = 0$, $\gamma = 0.1$, mesh Fig. 3a				

TABLE II

Node	1	26	51	13	38	63	25	50	75	301	26-50	51-1
Analytical °C	361.0	390.9	423.0	358.7	387.2	417.76	356.6	383.6	412.52	1853	7.304	61.9
FEM(linear)°C	360.7	387.9	416.8	358.7	384.8	412.5	356.8	381.7	408.2	1846.1	6.166	56.1
FEM (non-linear) °C	360.6	387.8	416.7	358.7	384.8	412.5	356.8	381.8	408.4	2105.0	5.981	56.0
$\alpha = 0.31$, $\gamma = 0.1$, mesh of Fig. 4												

TABLE III

Initial linear power	p(0)	440 W/cm
Tilt factor (steady state)	γ	0.1
Fuel radius	a	0.41 cm
Fuel density	ρ_1	10.4 g/cm^3
Fuel specific heat	C_1	0.315 J/g°C
Fuel thermal conductivity	λ_1	0.03 W/cm°C
Fuel/clad heat transfer coefficient	h_g	.5 W/cm^2°C
Clad thickness	b-a	0.06 cm
Clad density	ρ_2	6.6 g/cm^3
Clad specific heat	C_2	0.276 J/g°C
Clad thermal conductivity	λ_2	0.162 W/cm°C
Clad coefficient of thermal dilatation	β	6.5 10^{-6} °C^{-1}
Clad Elastic Young's Modulus	E	9.8 10^5 kg/cm^2

TABLE III a

Temperature-Dependent Fuel Conductivity

T °C	227	727	1227	1727	2227
UO_2 W/cm°C	.06	.0345	.0235	.023	.0165

TABLE IV

	Scram Curve $p(t) = \bar{p} \times 440$ W/cm	$T_m \equiv$ Coolant temp.	
time (sec)	$\bar{p}$: normalised power	Fast Blow down (°C)	Moderate Blow down (°C)
0	1.0	307	312
0.2	0.9265	307	312
0.4	0.7440	307	312
0.6	0.5901	302	312
0.8	0.4944	297	312
1	0.3414	292	310
2	0.1591	258	303
3	0.0973	228	299
4	0.0775	200	292
6	0.0638	128	271
8	0.0591	121	253
10	0.0545	112	230
12	0.05	106	202

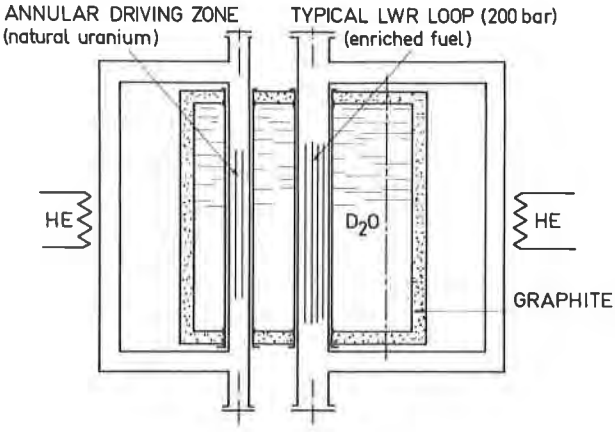

Fig.1 SKETCH OF ESSOR LWR LOOP

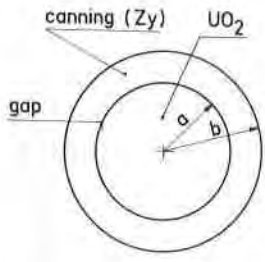

Fig 2 CROSS-SECTION OF FUEL PIN

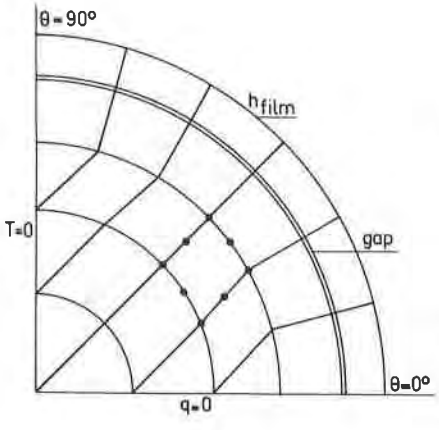

Fig. 3b MESH FOR FIRST ORDER FOURIER TERM

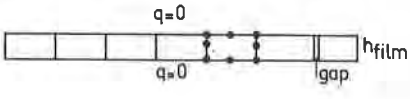

Fig 3a MESH FOR ZERO ORDER FOURIER TERM

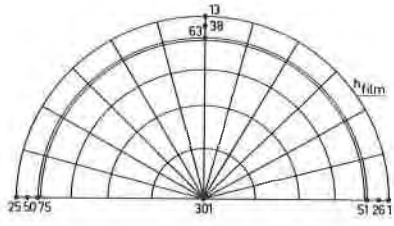

Fig 4 MESH FOR NON-LINEAR SOLUTION

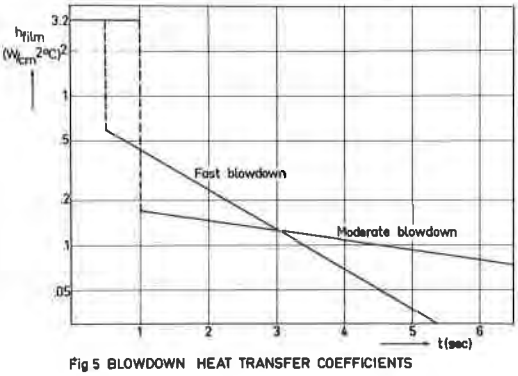

Fig 5 BLOWDOWN HEAT TRANSFER COEFFICIENTS

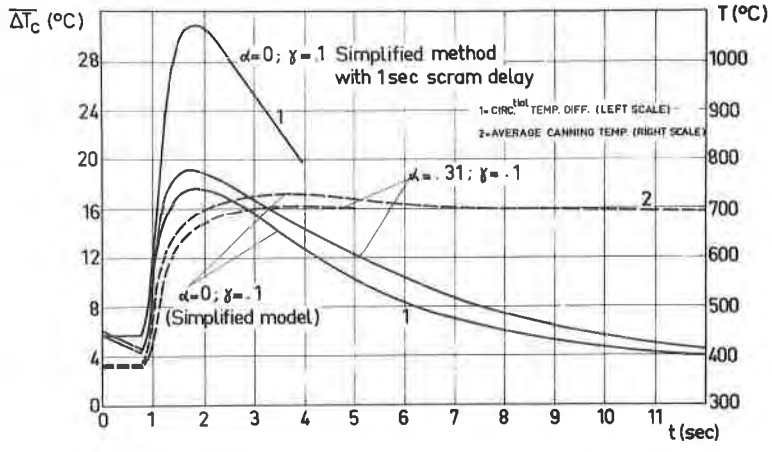

Fig.6 MODERATE BLOWDOWN

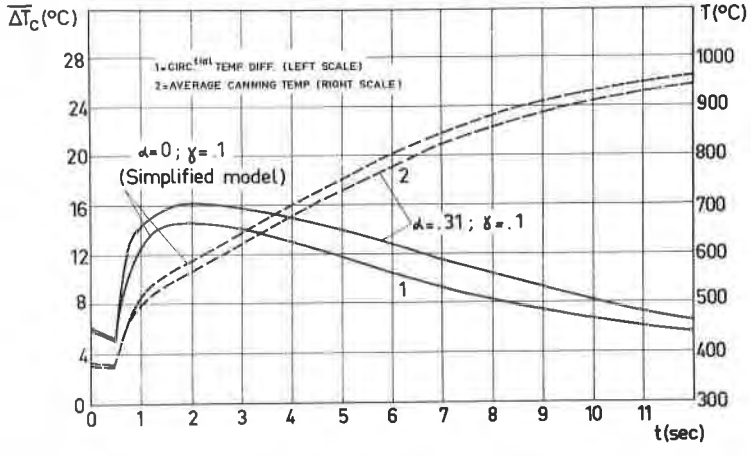

Fig.7 FAST BLOWDOWN